Redox Biology 28 (2020) 101356

Contents lists available at ScienceDirect

Redox Biology

journal homepage: www.elsevier.com/locate/redox

Hydrogen sulfide attenuates cigarette smoke-induced airway remodeling by upregulating SIRT1 signaling pathway

Ruijuan Guan[1], Jian Wang[1], Zhou Cai[1], Ziying Li, Lan Wang, Yuanyuan Li, Jingyi Xu, Defu Li, Hongwei Yao, Wei Liu, Bingxian Deng, Wenju Lu*

State Key Laboratory of Respiratory Diseases, Guangdong Key Laboratory of Vascular Diseases, National Clinical Research Center for Respiratory Diseases, Guangzhou Institute of Respiratory Health, The First Affiliated Hospital of Guangzhou Medical University, Guangzhou, Guangdong, China

ARTICLE INFO

Keywords:
Hydrogen sulfide
COPD
Airway remodeling
Oxidative stress
Epithelial-mesenchymal transition
Sirtuin 1

ABSTRACT

Airway remodeling is one of the characteristics for chronic obstructive pulmonary disease (COPD). The mechanism underlying airway remodeling is associated with epithelial-mesenchymal transition (EMT) in the small airways of smokers and patients with COPD. Sirtuin 1 (SIRT1) is able to reduce oxidative stress, and to modulate EMT. Here, we investigated the effects and mechanisms of hydrogen sulfide (H_2S) on pulmonary EMT *in vitro* and *in vivo*. We found that H_2S donor NaHS inhibited cigarette smoke (CS)-induced airway remodeling, EMT and collagen deposition in mouse lungs. In human bronchial epithelial 16HBE cells, NaHS treatment also reduced CS extract (CSE)-induced EMT, collagen deposition and oxidative stress. Mechanistically, NaHS upregulated SIRT1 expression, but inhibited activation of TGF-β1/Smad3 signaling *in vivo* and *in vitro*. SIRT1 inhibition by a specific inhibitor EX527 significantly attenuated or abolished the ability of NaHS to reverse the CSE-induced oxidative stress. SIRT1 inhibition also abolished the protection of NaHS against CSE-induced EMT. Moreover, SIRT1 activation attenuated CSE-induced EMT by modifying TGF-β1-mediated Smad3 transactivation. In conclusion, H_2S prevented CS-induced airway remodeling in mice by reversing oxidative stress and EMT, which was partially ameliorated by SIRT1 activation. These findings suggest that H_2S may have therapeutic potential for the prevention and treatment of COPD.

1. Introduction

Chronic obstructive pulmonary disease (COPD), a leading global cause of morbidity and mortality, is characterized by persistent airflow limitation that is progressive and not fully reversible [1]. Cigarette smoking is considered as the major risk factor for COPD and contributes to structural alterations in the airways during COPD progression [2]. Remodelled airways are characterized by an alteration in the epithelial injury, sub-epithelial thickening and fibrosis, goblet cell hyperplasia, airway smooth muscle proliferation, collagen deposition and reticular basement membrane thickening [3,4]. Bronchial epithelial cells are the first anatomical barrier exposed to noxious gases and particles of cigarette smoke (CS), which can initiate airway remodeling in COPD [5]. Airway epithelial-mesenchymal transition (EMT) is a highly plastic process through which epithelial cells change into a mesenchymal phenotype following epithelial damage. This results in the thickening of the wall of the airways. CS induces EMT in differentiated bronchial epithelial cells via release and autocrine action of transforming growth factor (TGF)-β1 as well as by enhancing oxidative stress [5]. Current available pharmacologic therapies, including corticosteroids, bronchodilators, phosphodiesterase-4 inhibitors and β2-agonists, are able to reduce exacerbations and improve symptoms but not to suppress the progression of this disease [6]. Hence, identification of the molecular mechanisms mediating EMT and exploration of the effective and safe strategies that could attenuated EMT might be beneficial for the prevention and therapy of COPD.

Abbreviations: α-SMA, α-smooth muscle actin; CAT, catalase; CK, Cytokeratin; COPD, chronic obstructive pulmonary disease; CS, cigarette smoke; CSE, cigarette smoke extract; EMT, epithelial-mesenchymal transition; FSP-1, fibroblast specific protein-1; H_2S, hydrogen sulfide; MDA, malondialdehyde; MMP, matrix metalloproteinase; NAC, N-Acetyl-L-cysteine; ROS, reactive oxygen species; SIRT1, Sirtuin 1; SOD2, superoxide dismutase 2; TGF-β1, transforming growth factor-β1; TGFβR1, TGF-β1 receptor type I

* Corresponding author. State Key Lab of Respiratory Diseases, Guangdong Key Laboratory of Vascular Diseases, Guangzhou Institute of Respiratory Health, The First Affiliated Hospital, Guangzhou Medical University, Guangzhou, China.
E-mail address: wlu92@qq.com (W. Lu).
[1] These authors contributed equally to this work.

https://doi.org/10.1016/j.redox.2019.101356
Received 29 July 2019; Received in revised form 14 October 2019; Accepted 21 October 2019
Available online 24 October 2019

The NAD^+-dependent deacetylase Sir2 was found to be a vital regulator of antioxidant genes [7]. Mammals have seven sirtuins paralogs (SIRT1-7), with Sirtuin (SIRT)1 being the closest to Sir2 [8]. SIRT1 is the best-characterized sirtuin among the seven and largely located in the lungs, which plays a pivotal role in many pathophysiological processes, including cellular senescence, inflammation, oxidative stress, and mitochondria dysfunction [9,10]. For instance, SIRT1 can regulate a stress-response transcription factor, FOXO3, thereby downregulating oxidative stress [10–12]. SIRT1 also regulates the RelA/p65 subunit of NF-kB, thereby protecting non-small cell lung cancer cells against osteopontin-induced EMT [13]. Rajendrasozhan and others have shown that SIRT1 is reduced in the lungs of smokers and patients with COPD [14,15], and activation of SIRT1 by SRT1720 protected against CS-induced emphysema in mice [10]. Thus, drugs that activate SIRT1 signaling might be beneficial in the prevention and treatment of CS-induced airway remodeling.

Hydrogen sulfide (H_2S), a gas that smells of rotten eggs, is generated endogenously in mammalian cells from L-cysteine mainly by key enzymes, for example, cystathionine c-lyase, cystathionine b-synthetase and 3-mercaptypyruvate sulfurtransferase [16]. Although high concentration of H_2S is toxic [17], endogenous H_2S has emerged as the third endogenous gaseous messenger that plays an important role in a variety of physiological processes [18]. Exogenous H_2S decreases coronary artery wall thickness in the spontaneously hypertensive rat by inhibiting reactive oxygen species (ROS) [19]. H_2S reduces oxidative stress in myocardial hypertrophy via a SIRT3-dependent manner [20]. H_2S inhibits TGF-β1-induced EMT in renal tubular epithelial cells via Wnt/catenin pathway [21]. H_2S also ameliorates chronic restrain stress-induced cognitive impairment in hippocampus by upregulating SIRT1 [22]. A recent study demonstrated that H_2S metabolism is altered in the lungs of smokers and COPD patients [23], and treatment with H_2S donor NaHS not only attenuates CS-induced emphysema in mice [24], but also reduces nicotine-induced endoplasmic reticulum stress and apoptosis in bronchial epithelial cells [25]. However, the effects of H_2S on CS-induced airway remodeling and the mechanism(s) involved are largely unknown.

We hypothesized that H_2S protects against airway remodeling by attenuating oxidative stress-induced EMT through the SIRT1 signaling pathway. To test this hypothesis, we examined the effects of NaHS on CS-induced bronchial remodeling and EMT in mice and on cigarette smoke extract (CSE)-induced EMT in bronchial epithelial 16HBE cells. The alterations in oxidative stress and the underlying involvement of the SIRT1 signaling pathway were also investigated.

2. Materials and methods

2.1. Chemicals and reagents

NaHS (Cat# 161527), and N-Acetyl-L-cysteine (NAC, Cat# A7250) were purchased from Sigma-Aldrich (St Louis, MO, USA). The cigarettes were purchased from Guangdong Tobacco Industry Co., Ltd. (Guangzhou, China). EX 527 (Cat# S1541) and SRT1720 (Cat# S1129) were purchased from Selleck Chemicals (Houston, TX, USA). The TRIzol Reagent was purchased from Ambion (Life Technologies, CA, USA). The PrimeScript RT reagent Kit with gDNA Eraser was from Takara Bio Inc. (Takara, Shiga, Japan), and the SsoFast EvaGreen Supermix was obtained from Bio-Rad Laboratories, Inc. (CA, USA). The antibodies used in this study include: anti-matrix metalloproteinase (MMP)-2 (Cat# 10373-2-AP), anti-MMP-9 (Cat# 10375-2-AP), anti-MMP-12 (Cat# 22989-1-AP), anti-fibronectin (Cat# 15613-1-AP), anti-TGF-β1 (Cat# 21898-1-AP) and anti-β-actin (Cat# 66009-1-Ig) polyclonal antibodies were purchased from Proteintech (Chicago, IL, USA); anti-Cytokeratin (CK)18 (Cat# GB11232), anti-collagen 1 (Cat# GB11022-2) and anti-collagen 3 (Cat# GB11023) polyclonal antibodies were purchased from Servicebio (Wuhan, China); anti-fibroblast specific protein (FSP)1 (Cat# A1631), and anti-superoxide dismutase (SOD)2 (Cat# A1340) antibodies were purchased from abclonal (Wuhan, China); anti-E-cadherin (Cat# 14472), anti-vimentin (Cat# 5741), anti-Snail (Cat# 3879), anti-SIRT1 (Cat# 8469), anti-p-Smad3 (Cat# 9520), and anti-Smad3 (Cat# 9523) antibodies were purchased from Cell Signaling Technology (CA, USA); anti-TGF-β1 receptor type I (TGFβR1) monoclonal antibody (Cat# AHO1552) was purchased from Thermo Fisher Scientific (Boston, MA, USA); anti-α-SMA antibody (Cat# ab32575) and the HRP-labeled Goat Anti-Rabbit/Mouse IgG (H + L) were purchased from Abcam Biotechnology (Cambridge, MA, USA). The poly-vinylidene fluoride (PVDF) membranes were obtained from Millipore Corporation (Billerica, MA, USA). ECL-Plus detection kit probed was purchased from Tanon Science & Technology Co., Ltd. (Shanghai, China). All other reagents were purchased from GBCBIO Technologies Inc. (Guangzhou, China) unless otherwise indicated.

2.2. Animals and treatments

Adult male C57BL/6J mice (18–20 g) were obtained from the Nanjing BioMedical Research Institute of Nanjing University (Nanjing, China), housed in a room at controlled temperature of 25 °C with 12/12 light/dark cycle, and allowed free access to diet and water ad libitum. Animal experimental protocol was approved by the Ethics Committee of the First Affiliated Hospital of Guangzhou Medical University. Mice were randomly allocated to one of three groups: 1) room air exposure plus atomization inhalation of sterile saline (control group); 2) CS exposure plus atomization inhalation of sterile saline (CS group); and 3) CS exposure plus atomization inhalation of NaHS (CS + NaHS group). For the CS-induced COPD mouse model, mice were placed in a 60 × 57 × 100 cm fume box and exposed to 9 filter-tipped cigarettes (tar: 13 mg/cigarette; nicotine:1.3 mg/cigarette) twice a day, 6 days per week. Each CS exposure lasted about 2 h with interval time between two CS exposures more than 4 h. The control animals were exposed to room air for 12 weeks. The sterile saline or NaHS (40 mg/kg, 30 min per session, twice per day) was administered via atomization inhalation 30 min before CS exposure. After all the mice were sacrificed, lungs were harvested for following experiments. In each animal experiment, there were 6 mice per group.

2.3. Masson's trichrome staining

Left lungs were fixed in 10% buffered formalin for 48 h and embedded in paraffin. Lung tissues were then cut into 3-μm-thick slices and stained with Masson's trichrome.

2.4. Immunohistochemistry

Immunohistochemistry was performed according to the method described as previously [26].

2.5. Cell culture

Human bronchial epithelial cells (16HBE) were obtained from Cell Bank of the Chinese Academy of Sciences (Shanghai, China), and cultured in Dulbecco's modified Eagle's medium (DMEM) containing 10% fetal bovine serum (FBS), 100 KU/L penicillin and 100 mg/L streptomycin in a humidified incubator at 37 °C with 5% CO_2 atmosphere. Each cell experiment was repeated at least three times.

2.6. Preparation of cigarette smoke extract (CSE)

CSE was freshly prepared from two filtered cigarettes into 10 ml DMEM within 30 min prior to treatments according to a previously described protocol [27].

2.7. Immunofluorescence staining

Cell immunofluorescence was performed as described previously [26]. Briefly, 16HBE cells were seeded on glass slides in 12-well plates and incubated as indicated for 48 h. The slides were washed three times with PBS, fixed in 4% paraformaldehyde for 10 min, and then permeabilized with 0.1% Triton X-100 for 20 min. Cells were then blocked with 3% BSA at room temperature for 1 h followed by incubation with a primary antibody E-cadherin (1:100 dilution) at 4 °C overnight. Slices were washed three times with PBS and incubated with a goat anti-mouse FITC-conjugated IgG (1:200 dilution, Cat# A0568, Beyotime Institute of Biotechnology, China) for 1 h, and then labeled with DAPI for 5 min. Finally, slices were washed four times with PBS, mounted in antifade mounting medium, and visualized and photographed under a fluorescence microscope (Olympus, BX53, Japan).

Lung sections (3 μm thickness) were deparaffinized and rehydrated. After antigen retrieval in citrate buffer with temperature 95–100 °C, tissues were blocked with 3% BSA and then incubated with mixed primary antibodies (E-cadherin and vimentin, 1:100 dilutions) at 4 °C overnight. After three-time washing with PBS, second antibodies, including goat anti-rabbit Cy3-conjugated IgG (1:200, Cat# A0516, Beyotime Institute of Biotechnology, China) and goat anti-mouse FITC-conjugated antibody (1:200, Cat# A0568, Beyotime Institute of Biotechnology, China), were incubated for 1 h and labeled with DAPI for 5 min. Finally, sections were washed four times with PBS and mounted in antifade mounting medium, and images were photographed under a fluorescence microscope (Olympus, BX53, Japan).

2.8. Measurement of intracellular ROS

Intracellular ROS production was detected using the DCFH-DA (Beyotime Institute of Biotechnology, China) with a fluorescence plate reader and fluorescence microscopy. Briefly, 16HBE cells were seeded in 12-well black plates and treated as indicated. After the medium was removed, cells were incubated with 1 ml of DCFH-DA solution (10 μM) at 37 °C for 20 min. Then cells were washed three times with warm serum-free DMEM, and the level of ROS was examined with a fluorescence microscope (EVOS™ Auto 2, Invitrogen, WA, USA).

2.9. Measurement of CAT and MDA levels

The malondialdehyde (MDA) and catalase (CAT) content was detected in the supernatant from 16HBE cells using MDA and CAT assay kits (Nanjing Jiancheng Bioengineering institute, Jiangsu, China) according to the manufacturer's instruction.

2.10. Measurement of GSH/GSSG

The ratio of reduced to oxidized glutathione was measured in the supernatant from 16HBE cells using GSH/GSSG kit (Beyotime Institute of Biotechnology, Jiangsu, China) according to the manufacturer's instruction.

2.11. Real-time PCR

Real-time PCR was performed as described previously [28]. Amplification was conducted using the following primers: 5'-GGGTGAGA CAGGCGAACAAG-3' (forward) and 5'- AACCAGCAGAGCCAGGGG-3' (reverse) for mouse Collagen 1, 5'- TGCCCACAGCCTTCTACACC-3' (forward) and 5'-GCCACCCATTCCTCCCAC-3' (reverse) for mouse Collagen 3, 5'-GCTGACGACTTCGACGACG-3' (forward) and 5'- TCGGTCA ACAGGAGGTTGTCT-3' (reverse) for mouse SIRT1, 5'-TAGCCTTGTCA GATAAGGAAGGA-3' (forward) and 5'-ACAGCTTCACAGTCAACTTTGT-3' (reverse) for human SIRT1, 5'-AAGGACCTCGGCTGGAAGTG-3' (forward) and 5'-CCGGGTTATGCTGGTTGTA-3' (reverse) for human TGF-β1, and 5'-GCAATTATTCCCCATGAACG-3' (forward) and 5'-GGCCTCA CTAAACCATCCAA-3' (reverse) for 18s.

2.12. Western blot

Equal amounts of protein from lung samples and 16HBE cells were used for Western blot [29]. Protein bands were scanned and quantified by using the Tanon-5200 infrared scanning system (anon Science & Technology Co., Ltd., Shanghai, China). The intensity analysis was analyzed by a densitometry system named Image J. The primary antibodies were as follows: mouse anti-E-cadherin antibody (1:1000 dilution), rabbit anti-CK18 antibody (1:1000 dilution), rabbit anti-fibronectin antibody (1:500 dilution), rabbit anti-vimentin antibody (1:1000 dilution), rabbit anti-α-SMA antibody (1:3000 dilution), rabbit anti-FSP-1 antibody (1:1000 dilution), rabbit anti-snail antibody (1:1000 dilution), rabbit anti-MMP-2 antibody (1:600 dilution), rabbit anti-MMP-9 antibody (1:600 dilution), rabbit anti-MMP-12 antibody (1:600 dilution), rabbit anti-TGF-β1 antibody (1:600 dilution), rabbit anti-TGFβR1 antibody (1:3000 dilution), rabbit anti-p-Smad3 antibody (1:1000 dilution), rabbit anti-Smad3 antibody (1:1000 dilution), rabbit anti-collagen 1 antibody (1:1000 dilution), rabbit anti-collagen 3 antibody (1:1000 dilution), mouse anti-SIRT1 antibody (1:1000 dilution), rabbit anti-SOD2 antibody (1:1000 dilution), and rabbit anti-β-actin antibody (1:3000 dilution). HRP-labeled Goat Anti-Rabbit IgG (H + L) (1:5000 dilution) and HRP-labeled Goat Anti-Mouse IgG (H + L) (1:5000 dilution) antibodies were used as secondary antibodies.

2.13. Data analysis

Data analysis was performed using SigmaPlot 12.5 (Systat Software, Inc., Chicago, IL, USA), and expressed as means ± SEM. Comparison of means among multiple groups was accomplished by one-way analysis of variance (ANOVA). A two-sided P value less than 0.05 ($P < 0.05$) were considered to be significantly different.

3. Results

3.1. H_2S donor NaHS attenuated CS-induced airway remodeling in mice

After 12 weeks of CS exposure, the mice developed an obvious airway remodeling phenotype, showing increased airway thickening and collagen deposition, as measured by Masson's trichrome staining. Treatment with NaHS significantly reduced CS-induced airway thickening and collagen deposition (Fig. 1A). Increased myofibroblast accumulation, characterized by elevated α-SMA and collagens, are phenotypic features for pathological airway remodeling [30]. Our results showed that the CS-induced upregulation of α-SMA, collagen 1 and collagen 3 levels were also attenuated by NaHS treatment (Fig. 1B–D). These results suggest that, for mice, NaHS reduces CS-induced airway remodeling.

3.2. H_2S donor NaHS inhibited EMT in CS-exposed mouse lungs

Increased differentiation of airway epithelial cells into mesenchymal cells, termed EMT, is one of the sources of myofibroblasts [31]. We, therefore, investigated whether the inhibition of airway remodeling by H_2S is due to the inhibition of EMT. Western blot analysis showed that CS significantly decreased E-cadherin and CK18 protein levels but increased fibronectin, vimentin, FSP-1 and α-SMA expressions, which were attenuated by NaHS treatment (Fig. 2A and B). Likewise, our immunofluorescence staining further demonstrated that the decreased fluorescence intensity of E-cadherin and increased vimentin fluorescence intensity induced by CS were reversed by NaHS treatment (Fig. 2C). Snail is considered as a main transcriptional repressor of E-Cadherin, we thus assessed its expression in response to NaHS treatment. The results showed that NaHS treatment significantly inhibited CS-induced Snail expression (Fig. 2A and B). In addition,

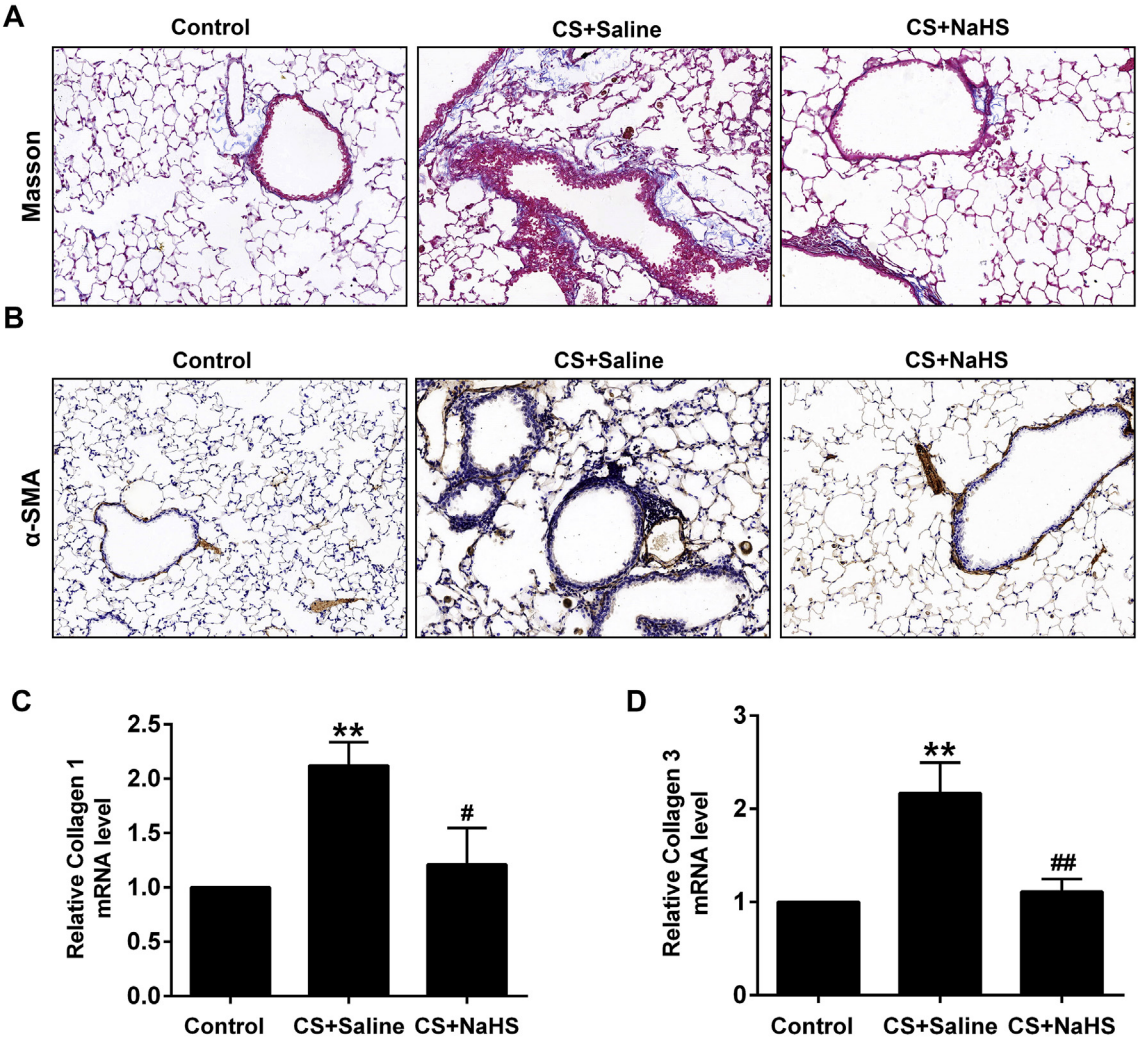

Fig. 1. NaHS attenuated cigarette smoke (CS)-induced airway remodeling in mice. After CS exposure for 12 weeks, mice were euthanized, and lung tissues were collected. (A) Masson's trichrome staining was performed to determined collagen deposition. Representative images from the lung sections of mice in the four groups. (B) Immunohistochemical staining for α-SMA was performed in the lungs. (C, D) The mRNA levels of collagen 1 and collagen 3 in the lungs were analyzed by Real-time PCR. Data are presented as mean ± SEM of 6 mice/group, **P < 0.01, significantly different from control group; #P < 0.05, ##P < 0.05, significantly different from CS + Saline group.

protein levels of MMP-2, MMP-9 and MMP-12, proteolytic enzymes that are the strong association with EMT, were also significantly decreased by NaHS treatment (Fig. 2 A, B).

CS can cause TGF-β1 release, activating its downstream signaling Smad2/3 cascade to promote small bronchi remodeling via EMT [32]. We therefore examined the effects of NaHS on CS-induced activation of TGF-β1 signaling. Our results showed that protein levels of TGF-β1 were dramatically increased in the CS-exposed mouse lungs, which was inhibited by NaHS treatment (Fig. 2D and 2E). TGF-β1 signaling cascade starts with TGF-β1 binding to TGF-β1 receptor type I (TGFβR1). We also evaluated the effect of NaHS on TGFβR1 expression. As shown in Fig. 2D and 2E, NaHS treatment also decreased CS-induced TGFβR1 expression in the lungs. Additionally, NaHS treatment inhibited CS-induced Smad3 phosphorylation (Fig. 2D and 2E). Altogether, the inactivation of TGF-β1 signaling is involved in the protective effect of NaHS on EMT in the CS-induced airway remodeling models.

3.3. H_2S donor NaHS reduced CSE-induced EMT and collagen deposition in bronchial epithelial 16HBE cells

We further assessed whether NaHS inhibits CSE-induced EMT using human bronchial epithelial 16HBE cells. Similar to our *in vivo* observations, treatment with NaHS repressed CSE-induced EMT, as indicated by the levels of protein markers for EMT (Fig. 3A–D). The inhibitory effects of NaHS on CSE-induced EMT were shown in a dose-dependent manner. Likewise, the reduced fluorescence intensity of E-cadherin induced by CSE was also increased by NaHS treatment (Fig. 3E). In addition, NaHS treatment significantly decreased CSE-induced upregulation of collagen 1 and collagen 3 levels, as compared to CSE alone treated cells (Fig. 3F–H). Moreover, the inhibitory effects of NaHS on TGF-β1/Smad3 signaling were also validated in human epithelial 16HBE cells (Fig. 3I–K).

3.4. H_2S donor NaHS decreased CSE-induced oxidative stress in 16HBE cells

Oxidative stress is highly correlated with the process of EMT [33]. In the present results, we found that treatment of 16HBE cells with the ROS scavenger NAC, inhibited CSE-induced upregulation of fibronectin, collagen 1 and collagen 3 protein expressions as well as the down-regulation of epithelial marker E-cadherin (Fig. 4A and 4B). This suggests that oxidative stress is involved in CSE-induced EMT in bronchial epithelial 16HBE cells. We therefore investigated the effects of NaHS on oxidative stress. As shown in Fig. 4C, CSE significantly elevated

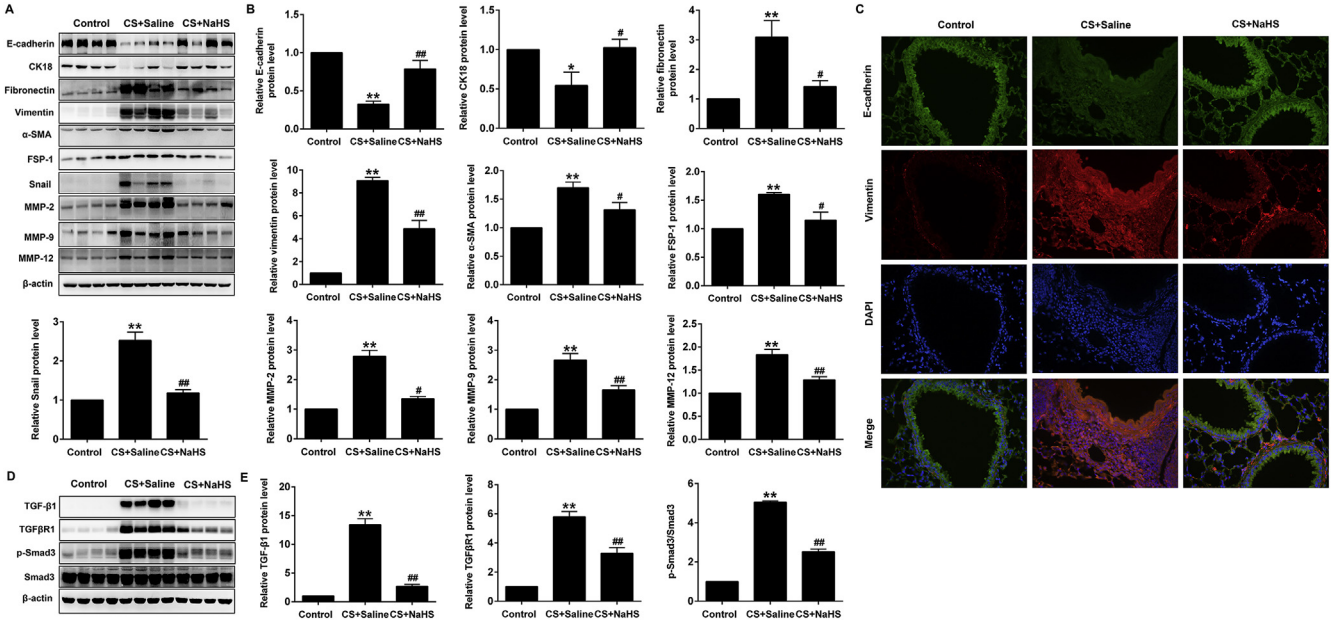

Fig. 2. NaHS inhibited EMT in CS-exposed mouse lungs. After CS exposure for 12 weeks, mice were euthanized, and lung tissues were collected. (A) Western blot was used to analyze the protein levels of E-cadherin, CK18, Fibronectin, vimentin, FSP-1, α-SMA, Snail, MMP-2, MMP-9 and MMP-12 in the lung tissues. (B) Densitometric analysis of E-cadherin, CK18, Fibronectin, vimentin, FSP-1, α-SMA, Snail, MMP-2, MMP-9 and MMP-12 in the immunoblots using β-actin as the internal reference. (C) The expression of E-cadherin and vimentin in the lungs were visualized using immunofluorescence double staining. (D, E) Western blot was used to analyze the protein levels of TGF-β1, TGFβR1 and p-Smad3 in mouse lungs. Data are presented as mean ± SEM of 6 mice/group, *P < 0.05, **P < 0.01, significantly different from control group; $^{\#}P < 0.05$, $^{\#\#}P < 0.01$, significantly different from CS + Saline group.

intracellular ROS levels, which were reduced by NaHS treatment. Moreover, the decreases in GSH/GSSG ratio and the activities of CAT, as well as the increases in MDA levels in CSE-treated 16HBE cells, were all significantly attenuated by NaHS treatment (Fig. 4D–F). Taken together, these data suggest that NaHS reduces CSE-induced oxidative stress in 16HBE cells.

3.5. Effects of NaHS on SIRT1 expression in CSE-stimulated 16HBE cells and in CS-exposed mouse lungs

SIRT1 plays a crucial role in many pathophysiological processes, including oxidative stress, mitochondria dysfunction and EMT [9,10,13]. We then investigated the involvement of SIRT1 in the protective effect of NaHS on EMT *in vivo* and *in vitro*, by examining the SIRT1 levels after CS exposure in the mice and CSE stimulation in the 16HBE cells. As shown in Fig. 5, the mRNA and protein levels of SIRT1 were significantly reduced in CS-exposed mouse lungs and in CSE-stimulated 16HBE cells. Expression of SIRT1 levels were restored to near or even higher than baseline by NaHS, as demonstrated by Real-time PCR and Western blot. These results indicate that SIRT1 might be involved in the protective effect of NaHS on EMT in the CS-induced airway remodeling models.

3.6. Effects of SIRT1 on the NaHS-mediated attenuation in CSE-induced oxidative stress and EMT in 16HBE cells

To further investigate the involvement of SIRT1 in the protective effect of NaHS in bronchial epithelial cells, we used a selective SIRT1 inhibitor, EX 527, to inhibit SIRT1.

We found that NaHS increased SOD2, CAT and GSH/GSSG ratio, but decreased intracellular ROS and MDA levels in CSE-treated 16HBE cells. These effects were abolished by EX 527 treatment (Fig. 6A–E), further suggesting NaHS suppressed oxidative stress via SIRT1 signaling. In addition, EX 527 abolished the inhibitory effect of NaHS on the expression of EMT-related proteins E-cadherin and α-SMA (Fig. 6F). Compared to NaHS treatment, the expression of E-cadherin decreased, whereas that of the mesenchymal protein α-SMA increased after EX 527 treatment. Therefore, SIRT1 may mediate the protection of NaHS against CSE-induced oxidative stress and EMT in bronchial epithelial cells.

3.7. SIRT1 reduced TGF-β1 signaling in the human 16HBE cells

Given the established role of SIRT1 and TGF-β1/Smad3 signaling in CSE-induced EMT, we further examined whether SIRT1 modulates TGF-β1-mediated Smad3 transactivation. Western blot showed that treatment of human 16HBE cells with TGF-β1 increased the phosphorylation level of Smad3, which was reduced by treatment of a specific SIRT1 activator, SRT1720 (Fig. 7A). In contrast, SIRT1 inhibition reversed these effects (Fig. 7B).

4. Discussion

The main and novel findings of the present study are that: (1) NaHS inhibited CS-induced myofibroblast accumulation, collagen deposition, and airway remodeling. (2) NaHS significantly upregulated the epithelial markers and decreased the mesenchymal markers *in vivo* and *in vitro* in response to CS exposure. (3) NaHS attenuated CSE-induced EMT by inhibiting oxidative stress in bronchial epithelial cells. (4) Protective effect of H_2S on oxidative stress-induced EMT was associated with enhancing SIRT1 signaling.

Cigarette smoking is able to cause airway remodeling and peribronchiolar fibrosis, leading to airway obstruction in patients with COPD [5]. During this process, EMT seems involved in the formation of peribronchiolar fibrosis, as demonstrated by lung bronchial fibroblasts originated directly from bronchial epithelial cells [34]. These gained fibroblasts not only contribute to fibrosis by releasing amounts of collagens, but also stimulate the epithelium to induce more EMT, which may form a vicious cycle for small airway narrowing and airflow obstruction [35]. In this regard, Sohal and colleagues have observed that airway biopsies from patients with COPD potentially undergo EMT [35]. Phenotypic markers of EMT are also observed in the bronchial

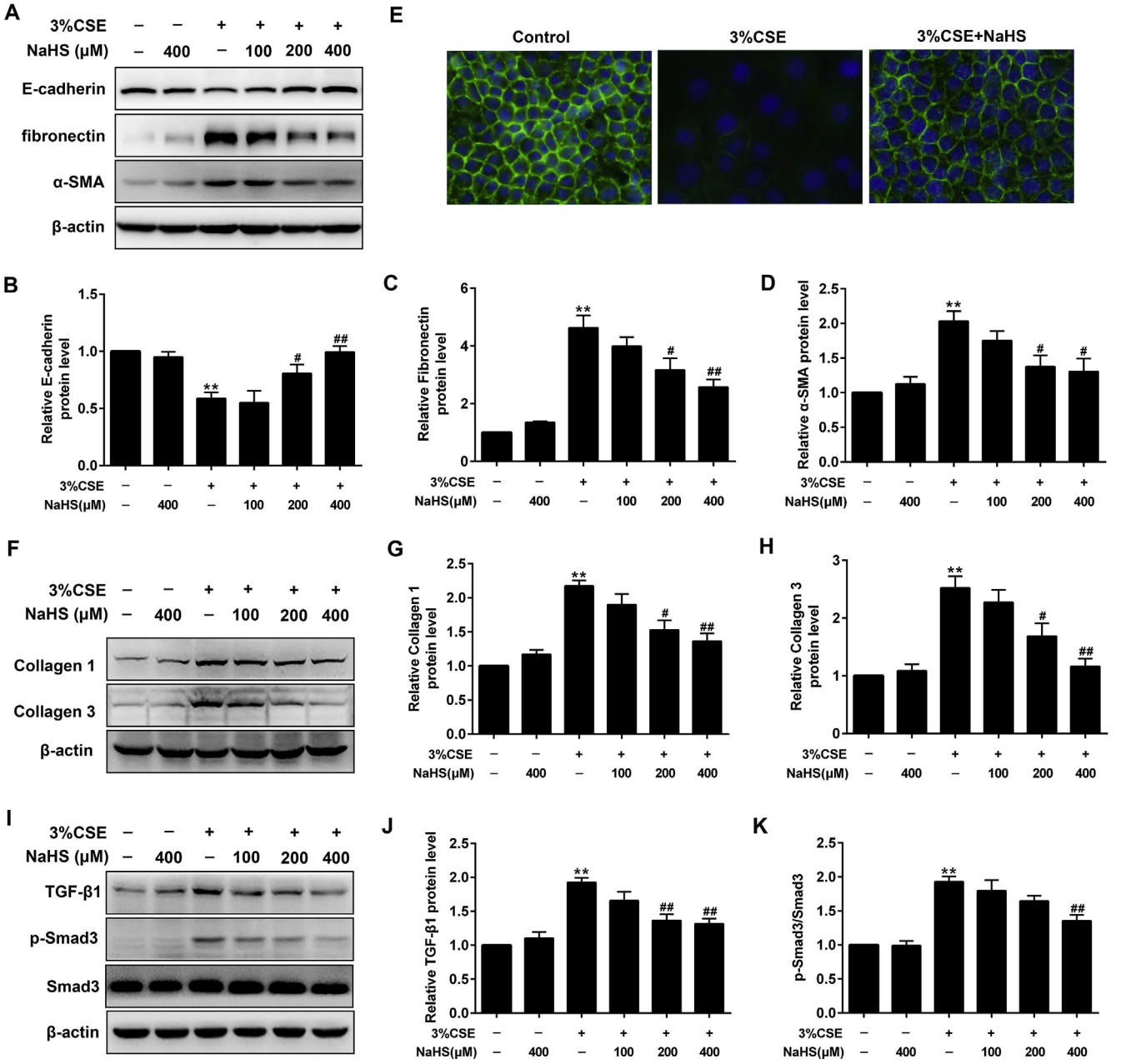

Fig. 3. NaHS repressed cigarette smoke extract (CSE)-induced EMT and collagen deposition in human bronchial epithelial 16HBE cells. (A) 16HBE cells were treated with 3% CSE and different concentrations of NaHS (100, 200, or 400 μM) for 48 h. The protein levels of E-cadherin, fibronectin and α-SMA was analyzed by Western blot. (B–D) Densitometric analysis of proteins of interest in the immunoblots using β-actin as the internal reference. (E) Immunofluorescence for E-cadherin was performed on human 16HBE cells treated with and without 3% CSE in the presence of 400 μM NaHS for 48 h. (F–H) Western blot was used to detect collagen 1 and collagen 3 levels. (I–K) Western blot was used to analyze the protein levels of TGF-β1 and p-Smad3. Data are presented as mean ± SEM of at least three independent experiments, **P < 0.01, significantly different from untreated cells [3%CSE (-) and NaHS (-)]; #P < 0.05, ##P < 0.01, significantly different from cells treated with CSE only.

epithelial cells of small bronchi from smokers and patients with COPD [5]. Thus, EMT is thought of as a fundamental underlying pathogenic process in COPD airways [36]. In this study, we found that both the mouse lungs and bronchial epithelial 16HBE cells undergo EMT in response to CS, as demonstrated by specific markers and phenotypic changes, which is consistent with previous findings that CS can induce EMT in alveolar type II cell line A549 [37], bronchial epithelial cell line BEAS2B [38], and primary human bronchial epithelial cells [5]. Whereas treatment with NaHS significantly inhibited EMT *in vivo* and *in vitro*, which is in agreement with previous observations that H_2S reduces EMT in alveolar epithelial cells, peritoneal mesothelial cells and renal tubular epithelial cells [39–41]. We also found that NaHS reduced CS-induced collagen deposition *in vivo* and *in vitro*. This is consistent with the previous findings that H_2S protects against the development of pulmonary fibrosis in rodents [42,43]. Thus, reduction of EMT may contribute to the protection of NaHS against CS-induced airway remodeling.

CS is able to activate TGF-β1-Smad2/3 pathway in bronchial rat explants, which is an essential signaling for EMT, leading to the formation of small bronchi remodeling [44]. CS also induces EMT in differentiated bronchial epithelial cells via the release and autocrine action of TGF-β1 [5]. Indeed, TGF-β1 levels in small airway epithelium from smokers and patients with COPD were significantly higher than that in non-smoker controls [45]. Furthermore, TGF-β1 mRNA levels

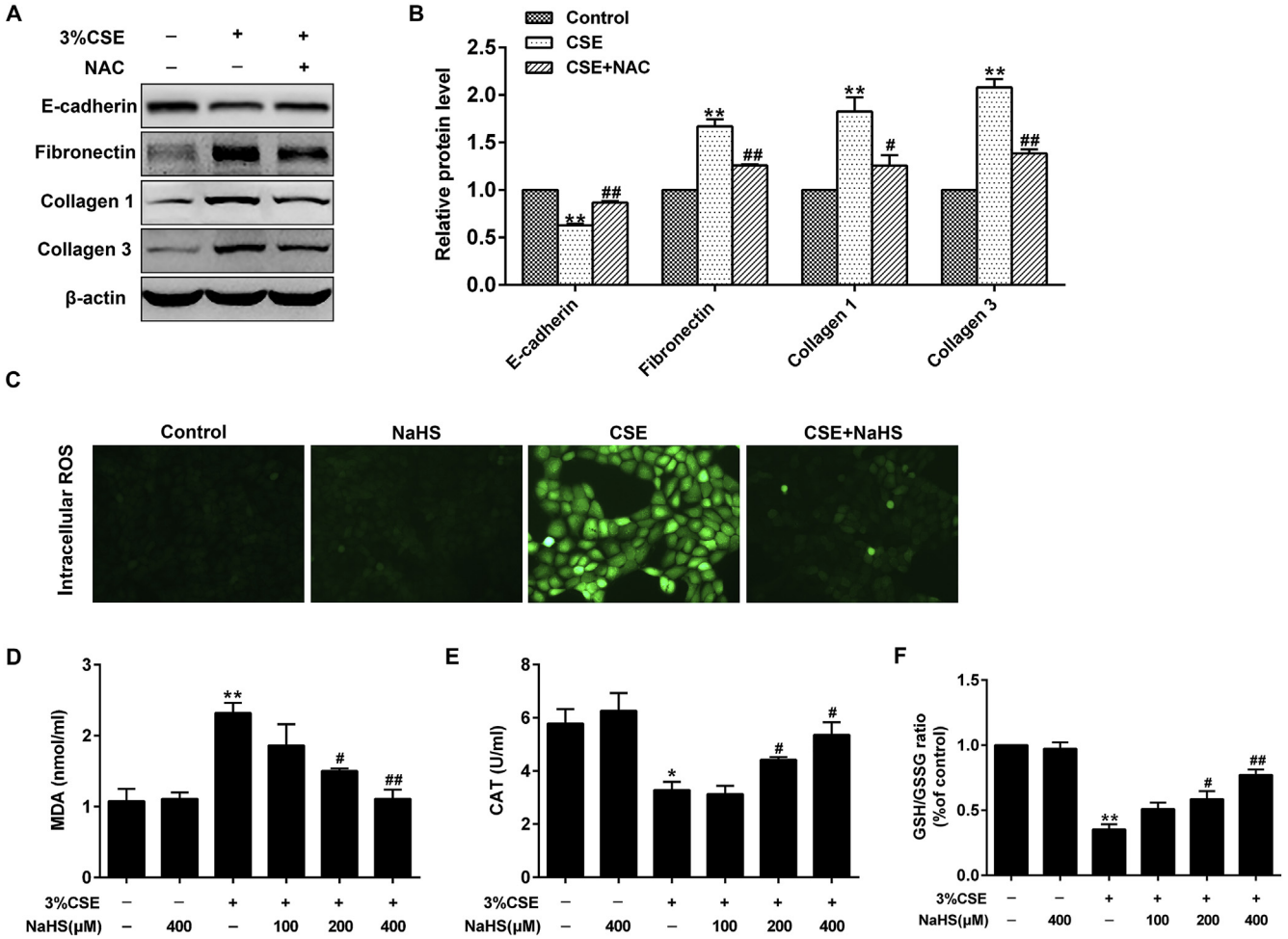

Fig. 4. NaHS reduced CSE-induced oxidative stress in human bronchial epithelial 16HBE cells. (A, B) 16HBE cells were incubated with 3% CSE and the ROS scavenger N-Acetyl-L-cysteine (NAC) for 48 h. Western blot was used to detect E-cadherin, fibronectin, Collagen 1 and Collagen 3 protein expressions. Data are presented as mean ± SEM of at least three independent experiments, **P < 0.01, significantly different from control cells [3%CSE (-) and NAC (-)]; $^{\#}P < 0.05$, $^{\#\#}P < 0.01$, significantly different from cells treated with CSE only. (C) 16HBE cells treated with and without 3%CSE in the absence or presence of 400 μM NaHS for 48 h. Representative microphotographs showing intracellular ROS. 16HBE cells were treated with 3% CSE and different concentrations of NaHS (100, 200, or 400 μM) for 48 h. (D) MDA levels. (E) Activities of CAT. (F) The GSH/GSSG ratio. Data are presented as mean ± SEM of at least three independent experiments, *P < 0.05, **P < 0.01, significantly different from untreated cells [3%CSE (-) and NaHS (-)]; $^{\#}P < 0.05$, $^{\#\#}P < 0.01$, significantly different from cells treated with CSE only.

correlated positively with the extent of pack-years and the degree of small airway obstruction among those smokers with COPD [45]. Thus, we investigated whether NaHS exerted its anti-EMT effect through the inactivation of key molecules in the TGF-β1 signaling. We found that NaHS treatment attenuated CS-induced activation of TGF-β1-Smad3 signaling pathway *in vivo* and *in vitro*. Therefore, H_2S ameliorates CS-induced bronchial remodeling by inhibiting EMT via the TGF-β1/Smad3 signaling. Further study is required to investigate whether NaHS affects other signaling pathways, including Wnt and ERK, which are involved in the EMT.

It has been shown that H_2S exerts pulmonary protective effects through its antioxidant properties. For instance, H_2S can reduce the production and accumulation of ROS and NOX2 in the lung after acute lung injury [46]. H_2S protected human bronchial epithelial cells against chemical hypoxia-induced injury via attenuation of ROS-mediated Ca^{2+} overload [47]. ROS can activate a wide variety of remodeling signaling kinases and transcription factors, which play a central role in the occurrence and development of bronchial remodeling. On the contrary, antioxidant defense systems play an important role in the maintenance of cellular redox homeostasis [48]. Our study found that NaHS protected against CSE-induced oxidative damage in bronchial epithelial cells, which was mediated via the reduction in ROS generation and the increases in antioxidant enzyme activities. Since H_2S has free radical scavenging capacity, it is probable that NaHS alleviates oxidative damage in bronchial epithelial cells by directly scavenging excessive ROS. Given the role of oxidative stress in the physiopathology of bronchial EMT, H_2S protects against CSE-induced bronchial EMT, at least in part, by inhibiting oxidative stress. Further study is required to determine whether NaHS specifically reduces CS-induced generation of cytosol and mitochondrial ROS.

We further analyzed the mechanisms through which H_2S attenuated cigarette smoke-induced EMT. SIRT1, an enzyme with de-acetylase activity, is a latent candidate that may contribute to the remodeling response [49]. Several evidences have suggested the reduced level and activity of SIRT1 in CS-exposed mouse lungs as well as in the lung of smokers and patients with COPD [10]. We found that NaHS treatment attenuated CS-induced reduction of SIRT1, and a SIRT1 inhibitor abolished the protection of NaHS against CS-induced EMT, which is in agreement with previous observations on the activity of SIRT1 in various cells and diseases. However, we noticed that the role of SIRT1 in EMT is sophisticated, with both pro- and anti-EMT effects. For instance, Rong and co-workers found that SIRT1 was significantly decreased in bleomycin (BLM)-induced pulmonary fibrosis, and treatment with SIRT1 activator alleviated the BLM-induced EMT in mice [50]. SIRT1

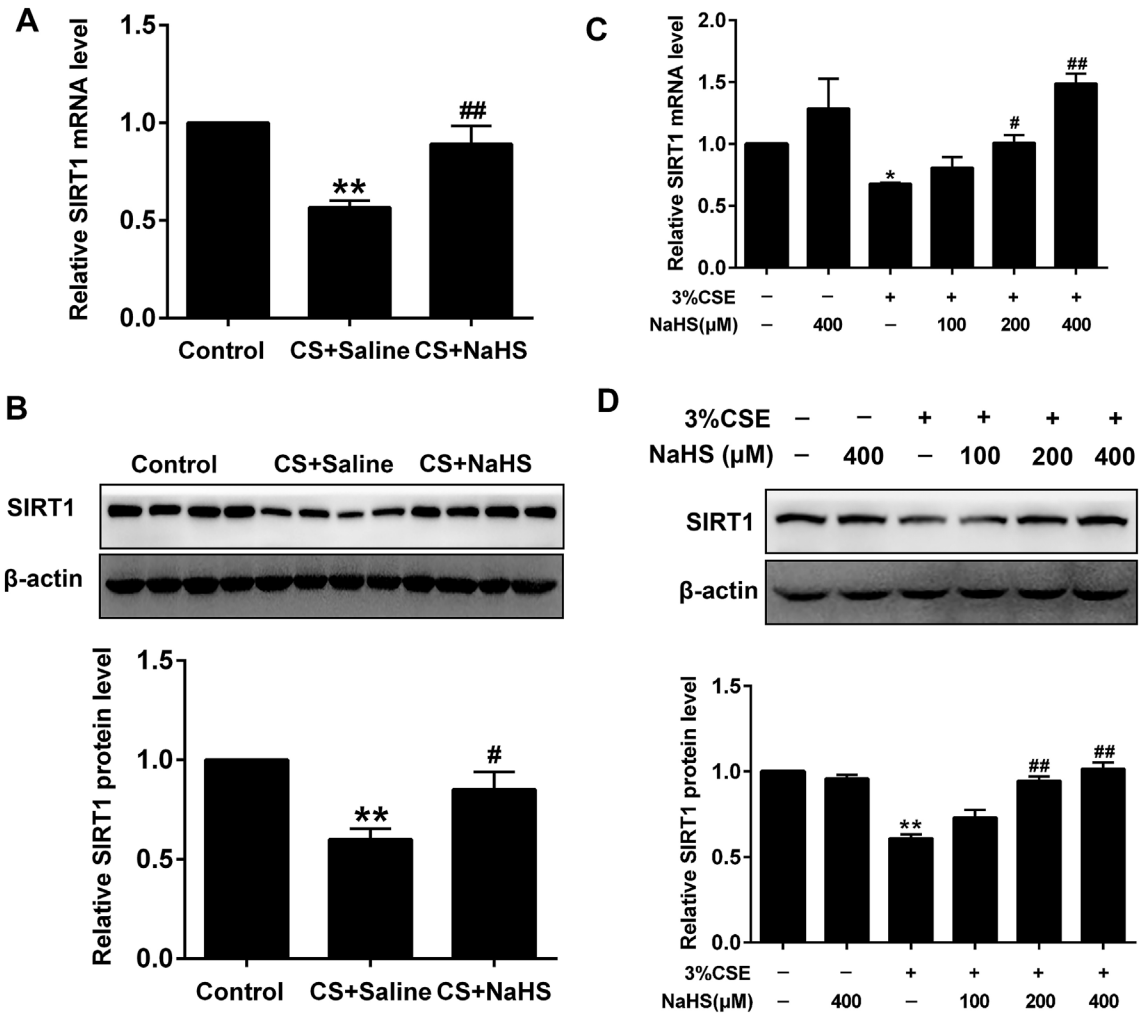

Fig. 5. Effects of NaHS on SIRT1 signaling in CSE-stimulated 16HBE cells and in CS-exposed mouse lungs. After CS exposure for 12 weeks, lung tissues were collected. (A) The SIRT1 mRNA level was detected by Real-time PCR. (B) The SIRT1 protein level was detected using Western blot. Data are presented as mean ± SEM of 6 mice/group, **P < 0.01, significantly different from control group; $^{\#}P < 0.05$, $^{\#\#}P < 0.01$, significantly different from CS + Saline group. 16HBE cells were cultured with and without 3% CSE and/or 100, 200, or 400 μM NaHS for 48 h. (C) The mRNA level of SIRT1 was detected using Real-time PCR. (D) The protein level of SIRT1 was analyzed by Western blot assay. Data are presented as mean ± SEM of at least three independent experiments, *P < 0.05, **P < 0.01, significantly different from control cells [3%CSE (-) and NaHS (-)]; #P < 0.05, ##P < 0.01, significantly different from cells treated with 3%CSE only.

expression was also reduced in osteopontin-treated NSCLC cell lines, and overexpression of SIRT1 inhibited the osteopontin-induced EMT via NF-κB signaling [13]. Conversely, the expression levels of SIRT1 were dramatically higher in osteosarcoma tissues than those in adjacent normal tissues, and SIRT1 silencing inhibited the EMT ability of osteosarcoma cells *in vitro* [51]. These contradictory results may be explained by the facts that different types of cells have differential responses to SIRT1, and suggest that an appropriate concentration of SIRT1 reduces EMT, while exorbitant concentration of SIRT1 cause increased EMT. Taken together, this data suggests that H_2S protects against bronchial EMT via activation of SIRT1.

Given oxidative stress could be possible downstream effects of SIRT1 in mediating the anti-EMT activity of H_2S. We also investigated whether H_2S protects against CS-induced oxidative stress via upregulation of SIRT1. It was demonstrated that treatment with SRT1720, a SIRT1 activator, could increase the antioxidant genes and enzymes and thus reduced CS-induced lung oxidative stress via a FOXO3-dependent manner [10]. Inversely, deficiency of SIRT1 increased oxidative stress in the lung [52]. Consistent with these observations, our results revealed that EX 527 treatment also abolished the protection of NaHS against CS-induced oxidative stress, demonstrating that SIRT1 is crucial in the reduction of oxidative stress by H_2S. These findings further suggest that SIRT1 activation mediated the H_2S-induced effects on CSE-induced EMT.

Here, we also investigate the effects of SIRT1 activation on TGF-β1 signaling. The results showed that treatment with a SIRT1 activator SRT1720 attenuated, whereas a SIRT1 inhibitor EX 527 aggravated, TGF-β1-mediated Smad3 phosphorylation in bronchial epithelial cells. This suggests Smad3 is a specific SIRT1 target and that pharmacological activation of SIRT1 may be a novel therapeutic strategy to prevent/reverse COPD via modifying TGF-β1 signaling. The reduction in Smad3 phosphorylation with SRT1720, is consistent with a reduction in canonical TGF-β1 signaling via inhibition of the well-described TGF-β1 auto-induction loop.

There are several limitations in our investigation. We did not investigate other factors, such as inflammatory response, goblet cell hyperplasia and mucus hypersecretion that are involved in bronchial remodeling after NaHS treatment. Both SIRT1 and TGF-β1 can mediate a variety of cellular processes, including proliferation, differentiation and apoptosis. This remains to be investigated in terms of NaHS treatment in future study. Furthermore, it is not clear whether NaHS still protects against CS-induced airway remodeling in SIRT1 knockout cells or mice.

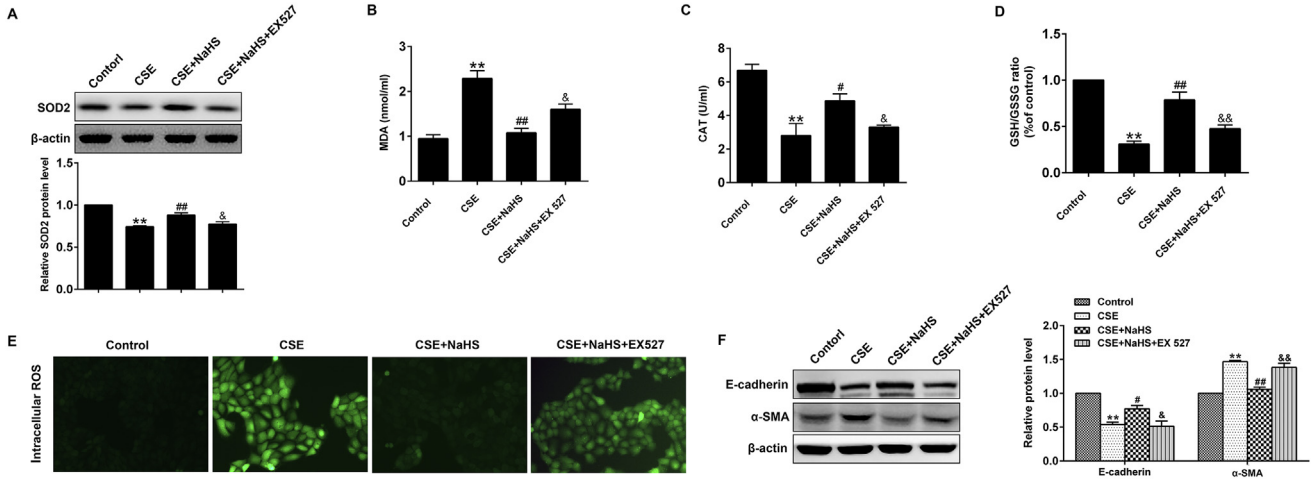

Fig. 6. Effects of SIRT1 on the NaHS-mediated attenuation in CSE-induced oxidative stress and EMT in 16HBE cells. 16HBE cells were cultured with SIRT1 inhibitor (EX527, 20 μM) in the absence and presence of 3% CSE and NaHS (400 μM) for 48 h. (A) The protein level of SOD2 was detected using Western blot. (B) MDA levels. (C) Activities of CAT (D) The GSH/GSSG ratio. (E) Representative microphotographs showing intracellular ROS generation. (F) Protein levels of E-cadherin and α-SMA were detected using Western blot. Data are presented as mean ± SEM of at least three independent experiments, **P < 0.01, significantly different from control cells; $^{\#}P < 0.05$, $^{\#\#}P < 0.01$, significantly different from cells treated with 3%CSE only; $^{\&}P < 0.05$, $^{\&\&}P < 0.01$, significantly different from cells treated with CSE and NaHS.

In conclusion, our results revealed that H_2S protects against CS-induced airway remodeling via the inhibition of TGF-β1-mediated EMT *in vivo* and *in vitro*. We found that the protective role of H_2S on EMT involves the suppression of oxidative stress via SIRT1 signaling. Our present study provides novel molecular mechanisms underlying the protective roles of H_2S against the development of COPD.

Author contributions

WL, RG and JW conceived the project and designed experiments. RG wrote the manuscript. JW, HY, ZC and ZL edited the manuscript. RG, CZ, ZL, LW, DL, YL, JX, and WLiu performed the experiments. RG, ZL, ZC and BD conducted data analysis. All authors have read and approved the final manuscript.

Declaration of competing interest

The authors have declared that there is no conflict of interest.

Acknowledgments

This work was supported by grants from the National Key R&D Program of China, China (2016YFC0903700 and 2016YFC1304102), the 973 Key Scheme of China (2015CB553406), China, the National Natural Science Foundation of China, China (81520108001, 81770043, 81800072 and 81220108001), Local Innovative and Research Teams Project of Guangdong Pearl River Talents Program, China (2017BT01S155), China Postdoctoral Science Foundation, China (2017M612637, 2018T110860), PhD Start-up Fund of Natural Science Foundation of Guangdong Province, China (2018A030310291), Changjiang Scholars and Innovative Research Team in University,

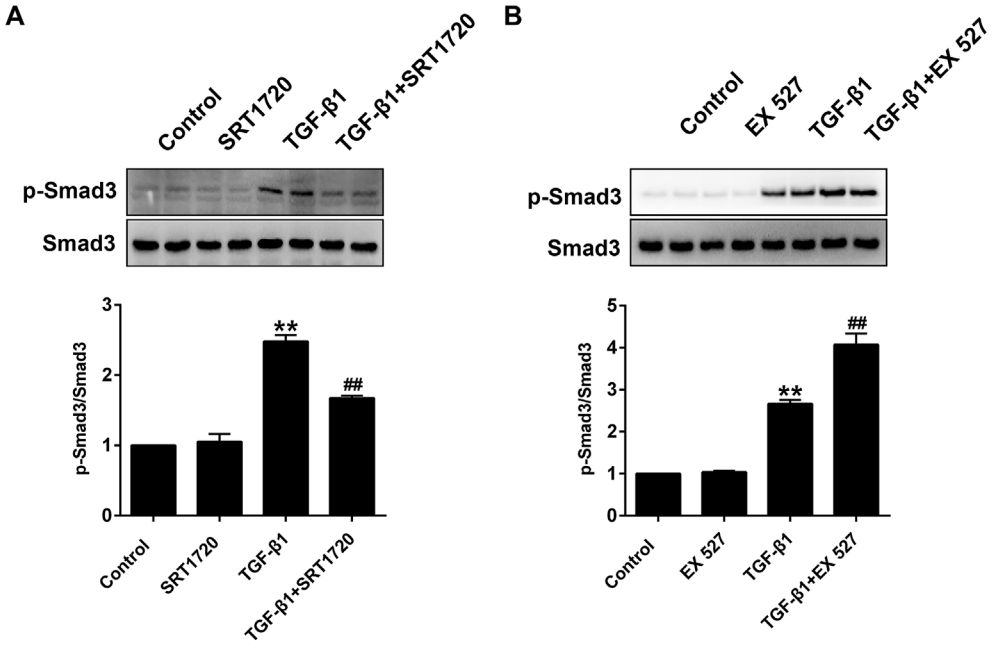

Fig. 7. SIRT1 attenuated canonical TGF-β1 signaling. (A) 16HBE cells were treated with TGF-β1 (5 ng/ml) in the presence or absence of the SIRT1 activator SRT1720. The protein level of p-Smad3 was analyzed by Western blot assay. (B) 16HBE cells were treated with TGF-β1 in the presence or absence of the SIRT1 inhibitor EX 527 (20 μM). The protein level of p-Smad3 was analyzed by Western blot assay. Data are presented as mean ± SEM of at least three independent experiments, **P < 0.01, significantly different from control cells; $^{\#\#}P < 0.01$, significantly different from cells treated with TGF-β1 only.

China grant IRT0961, Guangdong Department of Science and Technology, China grants (2016A030311020, 2016A030313606), Guangzhou Municipal Research Project, China (201607020030, 201804010052), Guangzhou Department of Education Innovation, China grant (1201620007), Project of State Key Laboratory of Respiratory Disease, China (SKLRD-OP-201808, SKLRD-QN-201706, SKLRD-QN-201917) and Guangdong Province Universities and Colleges Pearl River Scholar Funded Scheme, China (2014, for WL).

Appendix A. Supplementary data

Supplementary data to this article can be found online at https://doi.org/10.1016/j.redox.2019.101356.

Transparency document

Transparency document related to this article can be found online at https://doi.org/10.1016/j.redox.2019.101356.

References

[1] M. Szilasi, T. Dolinay, Z. Nemes, J. Strausz, Pathology of chronic obstructive pulmonary disease, Pathol. Oncol. Res. 12 (1) (2006) 52–60.
[2] J.I. Stewart, G.J. Criner, The small airways in chronic obstructive pulmonary disease: pathology and effects on disease progression and survival, Curr. Opin. Pulm. Med. 19 (2) (2013) 109–115.
[3] Y. Wang, M. Jia, X. Yan, L. Cao, P.J. Barnes, I.M. Adcock, M. Huang, X. Yao, Increased neutrophil gelatinase-associated lipocalin (NGAL) promotes airway remodelling in chronic obstructive pulmonary disease, Clin. Sci. (Lond.) 131 (11) (2017) 1147–1159.
[4] N. Hirota, J.G. Martin, Mechanisms of airway remodeling, Chest 144 (3) (2013) 1026–1032.
[5] J. Milara, T. Peiro, A. Serrano, J. Cortijo, Epithelial to mesenchymal transition is increased in patients with COPD and induced by cigarette smoke, Thorax 68 (5) (2013) 410–420.
[6] Y. Tian, J. Li, Y. Li, Y. Dong, F. Yao, J. Mao, L. Li, L. Wang, S. Luo, M. Wang, Effects of Bufei Yishen granules combined with acupoint sticking therapy on pulmonary surfactant proteins in chronic obstructive pulmonary disease rats, Biomed. Res. Int., 2016 (2016) 8786235.
[7] Y. Zhao, P. Luo, Q. Guo, S. Li, L. Zhang, M. Zhao, H. Xu, Y. Yang, W. Poon, Z. Fei, Interactions between SIRT1 and MAPK/ERK regulate neuronal apoptosis induced by traumatic brain injury in vitro and in vivo, Exp. Neurol. 237 (2) (2012) 489–498.
[8] M.C. Haigis, L.P. Guarente, Mammalian sirtuins–emerging roles in physiology, aging, and calorie restriction, Genes Dev. 20 (21) (2006) 2913–2921.
[9] X. Ou, M.R. Lee, X. Huang, S. Messina-Graham, H.E. Broxmeyer, SIRT1 positively regulates autophagy and mitochondria function in embryonic stem cells under oxidative stress, Stem Cells 32 (5) (2014) 1183–1194.
[10] H. Yao, S. Chung, J.W. Hwang, S. Rajendrasozhan, I.K. Sundar, D.A. Dean, M.W. McBurney, L. Guarente, W. Gu, M. Ronty, et al., SIRT1 protects against emphysema via FOXO3-mediated reduction of premature senescence in mice, J. Clin. Investig. 122 (6) (2012) 2032–2045.
[11] Y.S. Hori, A. Kuno, R. Hosoda, Y. Horio, Regulation of FOXOs and p53 by SIRT1 modulators under oxidative stress, PLoS One 8 (9) (2013) e73875.
[12] H.N. Kim, L. Han, S. Iyer, R. de Cabo, H. Zhao, C.A. O'Brien, S.C. Manolagas, M. Almeida, Sirtuin1 suppresses osteoclastogenesis by deacetylating FoxOs, Mol. Endocrinol. 29 (10) (2015) 1498–1509.
[13] X. Li, Z. Jiang, X. Li, X. Zhang, SIRT1 overexpression protects non-small cell lung cancer cells against osteopontin-induced epithelial-mesenchymal transition by suppressing NF-kappaB signaling, OncoTargets Ther. 11 (2018) 1157–1171.
[14] S. Rajendrasozhan, S.R. Yang, V.L. Kinnula, I. Rahman, SIRT1, an antiinflammatory and antiaging protein, is decreased in lungs of patients with chronic obstructive pulmonary disease, Am. J. Respir. Crit. Care Med. 177 (8) (2008) 861–870.
[15] Y. Nakamaru, C. Vuppusetty, H. Wada, J.C. Milne, M. Ito, C. Rossios, M. Elliot, J. Hogg, S. Kharitonov, H. Goto, et al., A protein deacetylase SIRT1 is a negative regulator of metalloproteinase-9, FASEB J. 23 (9) (2009) 2810–2819.
[16] R. Wang, Two's company, three's a crowd: can H2S be the third endogenous gaseous transmitter? FASEB J. 16 (13) (2002) 1792–1798.
[17] G. Meng, Y. Ma, L. Xie, A. Ferro, Y. Ji, Emerging role of hydrogen sulfide in hypertension and related cardiovascular diseases, Br. J. Pharmacol. 172 (23) (2015) 5501–5511.
[18] L.F. Hu, P.T. Wong, P.K. Moore, J.S. Bian, Hydrogen sulfide attenuates lipopolysaccharide-induced inflammation by inhibition of p38 mitogen-activated protein kinase in microglia, J. Neurochem. 100 (4) (2007) 1121–1128.
[19] Y.X. Shi, Y. Chen, Y.Z. Zhu, G.Y. Huang, P.K. Moore, S.H. Huang, T. Yao, Y.C. Zhu, Chronic sodium hydrosulfide treatment decreases medial thickening of intramyocardial coronary arterioles, interstitial fibrosis, and ROS production in spontaneously hypertensive rats, Am. J. Physiol. Heart Circ. Physiol. 293 (4) (2007) H2093–H2100.
[20] G. Meng, J. Liu, S. Liu, Q. Song, L. Liu, L. Xie, Y. Han, Y. Ji, Hydrogen sulfide pretreatment improves mitochondrial function in myocardial hypertrophy via a SIRT3-dependent manner, Br. J. Pharmacol. 175 (8) (2018) 1126–1145.
[21] L. Guo, W. Peng, J. Tao, Z. Lan, H. Hei, L. Tian, W. Pan, L. Wang, X. Zhang, Hydrogen sulfide inhibits transforming growth factor-beta1-induced EMT via Wnt/Catenin pathway, PLoS One 11 (1) (2016) e147018.
[22] X.N. Li, L. Chen, B. Luo, X. Li, C.Y. Wang, W. Zou, P. Zhang, Y. You, X.Q. Tang, Hydrogen sulfide attenuates chronic restrain stress-induced cognitive impairment by upregulation of Sirt1 in hippocampus, Oncotarget 8 (59) (2017) 100396–100410.
[23] Y. Sun, K. Wang, M.X. Li, W. He, J.R. Chang, C.C. Liao, F. Lin, Y.F. Qi, R. Wang, Y.H. Chen, Metabolic changes of H2S in smokers and patients of COPD which might involve in inflammation, oxidative stress and steroid sensitivity, Sci. Rep. 5 (2015) 14971.
[24] W. Han, Z. Dong, C. Dimitropoulou, Y. Su, Hydrogen sulfide ameliorates tobacco smoke-induced oxidative stress and emphysema in mice, Antioxidants Redox Signal. 15 (8) (2011) 2121–2134.
[25] F. Lin, C. Liao, Y. Sun, J. Zhang, W. Lu, Y. Bai, Y. Liao, M. Li, X. Ni, Y. Hou, et al., Hydrogen sulfide inhibits cigarette smoke-induced endoplasmic reticulum stress and apoptosis in bronchial epithelial cells, Front. Pharmacol. 8 (2017) 675.
[26] R. Guan, X. Wang, X. Zhao, N. Song, J. Zhu, J. Wang, J. Wang, C. Xia, Y. Chen, D. Zhu, et al., Emodin ameliorates bleomycin-induced pulmonary fibrosis in rats by suppressing epithelial-mesenchymal transition and fibroblast activation, Sci. Rep. 6 (2016) 35696.
[27] D. Li, J. Wang, D. Sun, X. Gong, H. Jiang, J. Shu, Z. Wang, Z. Long, Y. Chen, Z. Zhang, et al., Tanshinone IIA sulfonate protects against cigarette smoke-induced COPD and down-regulation of CFTR in mice, Sci. Rep. 8 (1) (2018) 376.
[28] R. Guan, J. Wang, Z. Li, M. Ding, D. Li, G. Xu, T. Wang, Y. Chen, Q. Yang, Z. Long, et al., Sodium tanshinone IIA sulfonate decreases cigarette smoke-induced inflammation and oxidative stress via blocking the activation of MAPK/HIF-1alpha signaling pathway, Front. Pharmacol. 9 (2018) 263.
[29] R. Guan, X. Zhao, X. Wang, N. Song, Y. Guo, X. Yan, L. Jiang, W. Cheng, L. Shen, Emodin alleviates bleomycin-induced pulmonary fibrosis in rats, Toxicol. Lett. 262 (2016) 161–172.
[30] H. Xu, M. Ling, J. Xue, X. Dai, Q. Sun, C. Chen, Y. Liu, L. Zhou, J. Liu, F. Luo, et al., Exosomal microRNA-21 derived from bronchial epithelial cells is involved in aberrant epithelium-fibroblast cross-talk in COPD induced by cigarette smoking, Theranostics 8 (19) (2018) 5419–5433.
[31] C.J. Scotton, R.C. Chambers, Molecular targets in pulmonary fibrosis: the myofibroblast in focus, Chest 132 (4) (2007) 1311–1321.
[32] R.D. Wang, J.L. Wright, A. Churg, Transforming growth factor-beta1 drives airway remodeling in cigarette smoke-exposed tracheal explants, Am. J. Respir. Cell Mol. Biol. 33 (4) (2005) 387–393.
[33] P. He, Z. Li, Z. Yue, H. Gao, G. Feng, P. Wang, Y. Huang, W. Luo, H. Hong, L. Liang, et al., SIRT3 prevents angiotensin II-induced renal tubular epithelial-mesenchymal transition by ameliorating oxidative stress and mitochondrial dysfunction, Mol. Cell. Endocrinol. 460 (2018) 1–13.
[34] S.S. Sohal, D. Reid, A. Soltani, C. Ward, S. Weston, H.K. Muller, R. Wood-Baker, E.H. Walters, Reticular basement membrane fragmentation and potential epithelial mesenchymal transition is exaggerated in the airways of smokers with chronic obstructive pulmonary disease, Respirology 15 (6) (2010) 930–938.
[35] S.S. Sohal, D. Reid, A. Soltani, C. Ward, S. Weston, H.K. Muller, R. Wood-Baker, E.H. Walters, Evaluation of epithelial mesenchymal transition in patients with chronic obstructive pulmonary disease, Respir. Res. 12 (2011) 130.
[36] K. Nowrin, S.S. Sohal, G. Peterson, R. Patel, E.H. Walters, Epithelial-mesenchymal transition as a fundamental underlying pathogenic process in COPD airways: fibrosis, remodeling and cancer, Expert Rev. Respir. Med. 8 (5) (2014) 547–559.
[37] Y. Liu, W. Gao, D. Zhang, Effects of cigarette smoke extract on A549 cells and human lung fibroblasts treated with transforming growth factor-beta1 in a co-culture system, Clin. Exp. Med. 10 (3) (2010) 159–167.
[38] E. Veljkovic, J. Jiricny, M. Menigatti, H. Rehrauer, W. Han, Chronic exposure to cigarette smoke condensate in vitro induces epithelial to mesenchymal transition-like changes in human bronchial epithelial cells, BEAS-2B, Toxicol. In Vitro 25 (2) (2011) 446–453.
[39] Y.W. Bai, M.J. Ye, D.L. Yang, M.P. Yu, C.F. Zhou, T. Shen, Hydrogen sulfide attenuates paraquat-induced epithelial-mesenchymal transition of human alveolar epithelial cells through regulating transforming growth factor-beta1/Smad2/3 signaling pathway, J. Appl. Toxicol. 39 (3) (2019) 432–440.
[40] S. Cheng, Y. Lu, Y. Li, L. Gao, H. Shen, K. Song, Hydrogen sulfide inhibits epithelial-mesenchymal transition in peritoneal mesothelial cells, Sci. Rep. 8 (1) (2018) 5863.
[41] Y. Huang, Z. Zhang, Y. Huang, Z. Mao, X. Yang, Y. Nakamura, N. Sawada, T. Mitsui, M. Takeda, J. Yao, Induction of inactive TGF-beta1 monomer formation by hydrogen sulfide contributes to its suppressive effects on Ang II- and TGF-beta1-induced EMT in renal tubular epithelial cells, Biochem. Biophys. Res. Commun. 501 (2) (2018) 534–540.
[42] H. Cao, X. Zhou, J. Zhang, X. Huang, Y. Zhai, X. Zhang, L. Chu, Hydrogen sulfide protects against bleomycin-induced pulmonary fibrosis in rats by inhibiting NF-kappaB expression and regulating Th1/Th2 balance, Toxicol. Lett. 224 (3) (2014) 387–394.
[43] X. Zhou, G. An, J. Chen, Inhibitory effects of hydrogen sulphide on pulmonary fibrosis in smoking rats via attenuation of oxidative stress and inflammation, J. Cell Mol. Med. 18 (6) (2014) 1098–1103.
[44] R.D. Wang, J.L. Wright, A. Churg, Transforming growth factor-beta1 drives airway remodeling in cigarette smoke-exposed tracheal explants, Am. J. Resp. Cell. Mol. 33 (4) (2005) 387–393.
[45] H. Takizawa, M. Tanaka, K. Takami, T. Ohtoshi, K. Ito, M. Satoh, Y. Okada, F. Yamasawa, K. Nakahara, A. Umeda, Increased expression of transforming growth

factor-beta1 in small airway epithelium from tobacco smokers and patients with chronic obstructive pulmonary disease (COPD), Am. J. Resp. Crit. Care 163 (6) (2001) 1476–1483.
[46] K.K. Zimmermann, S.G. Spassov, K.M. Strosing, P.M. Ihle, H. Engelstaedter, A. Hoetzel, S. Faller, Hydrogen sulfide exerts anti-oxidative and anti-inflammatory effects in acute lung injury, Inflammation 41 (1) (2018) 249–259.
[47] C.X. Liu, Y.R. Tan, Y. Xiang, C. Liu, X.A. Liu, X.Q. Qin, Hydrogen sulfide protects against chemical hypoxia-induced injury via attenuation of ROS-mediated Ca(2+) overload and mitochondrial dysfunction in human bronchial epithelial cells, Biomed. Res. Int., 2018 (2018) 2070971.
[48] Y. Huang, X. Zhu, K. Chen, H. Lang, Y. Zhang, P. Hou, L. Ran, M. Zhou, J. Zheng, L. Yi, et al., Resveratrol prevents sarcopenic obesity by reversing mitochondrial dysfunction and oxidative stress via the PKA/LKB1/AMPK pathway, Aging (N Y) 11 (8) (2019) 2217–2240.
[49] L. Guarente, H. Franklin, Epstein lecture: sirtuins, aging, and medicine, N. Engl. J. Med. 364 (23) (2011) 2235–2244.
[50] L. Rong, J. Wu, W. Wang, R.P. Zhao, X.W. Xu, D. Hu, Sirt 1 activator attenuates the bleomycin-induced lung fibrosis in mice via inhibiting epithelial-to-mesenchymal transition (EMT), Eur. Rev. Med. Pharmacol. Sci. 20 (10) (2016) 2144–2150.
[51] X.J. Yu, X.Z. Guo, C. Li, Y. Chong, T.N. Song, J.F. Pang, M. Shao, SIRT1-ZEB1-positive feedback promotes epithelial-mesenchymal transition process and metastasis of osteosarcoma, J. Cell. Biochem. 120 (3) (2019) 3727–3735.
[52] H. Yao, I.K. Sundar, T. Ahmad, C. Lerner, J. Gerloff, A.E. Friedman, R.P. Phipps, P.J. Sime, M.W. McBurney, L. Guarente, et al., SIRT1 protects against cigarette smoke-induced lung oxidative stress via a FOXO3-dependent mechanism, Am. J. Physiol. Lung Cell Mol. Physiol. 306 (9) (2014) L816–L828.